ChemCatChem

Research Article
doi.org/10.1002/cctc.202201048

Chemistry Europe
European Chemical Societies Publishing

www.chemcatchem.org

Special Collection

# Ligand Assisted $CO_2$ Activation and Catalytic Valorization by an NHI-Stabilized Stannylene

Debotra Sarkar[+],[a] Lisa Groll[+],[a] Dominik Munz,*[b, c] Franziska Hanusch,[a] and Shigeyoshi Inoue*[a]

The aryl(imino)stannylene $^{Mes}$Ter[N(IDipp)]Sn could be obtained by treating NHILi (NHI = N(IDipp), IDipp = C[N-(2,6-$^{i}$Pr$_2$C$_6$H$_3$)CH]$_2$) with $^{Mes}$TerSnCl ($^{Mes}$Ter = 2,6-Mes$_2$C$_6$H$_3$) and offers a unique reactivity pattern compared to conventional single site tetrylene catalyzed $CO_2$ reduction reactions. The Sn(II) center, stabilized by the NHI ligand enabled the sequestration and valorization of $CO_2$ to C1 feedstock stoichiometrically, as well as catalytically, utilizing HBpin (pin = pinacolato) as reductant. The experimental comparison with aryl(amido)stannylene $^{Mes}$Ter(NPh$_2$)Sn and aryl(phosphinidene)stannylene $^{Mes}$Ter[P(IDipp)]Sn, as well as computational analysis, rationalize the electronic features and key role of the NHI ligand in the $CO_2$ reduction process. In case of the phosphorus congener, Sn–P bonding with pronounced double-bond character is obtained, which prevents swift dissociation, thus preventing $CO_2$ uptake. Instead, hard/soft mismatch between tin and the NHI induces zwitterionic and single-bond character, switching on the intermediate dissociation of Sn(II)/NHI, followed by a tin hydride mediated reduction step, and thus allows for efficient catalysis under mild conditions.

## Introduction

$CO_2$ is ubiquitous in our environment and therefore presents an attractive resource for value-added C1 feedstock, especially in the face of current challenges associated with climate change and increasing global energy demands.[1] A lot of efforts to activate this thermodynamically robust molecule have been made. Frequently, transition-metal complexes with dynamic oxidation state variability, usually in redox-based mechanisms are applied, but also the use metal free systems and main group complexes, has been reported.[2] Particularly, the use of low valent p-block compounds in small molecule (*e.g.* $CO_2$) activation and catalysis has made great progress in recent years.[2a,c,3] In this context, low valent heavier group 14 carbene homologues, namely tetrylenes [R$_2$E:] (E = Si, Ge, Sn), which are in the +II oxidation state, gave new impetus.[3b,4] While silylene, germylene and stannylene mediated $CO_2$ activation is known, their catalytic application in $CO_2$ conversion is still scarce.[4l] The main challenge for utilizing tetrylenes in redox-based catalysis is enabling reductive elimination, and thereby release of the functionalized substrates.[2c,5]

An elegant approach to circumvent this challenge is reversible metal–ligand σ-bond cleavage and subsequent valorization to commodity chemicals. Here, the spatial proximity between nucleophilic and electrophilic reaction sites of ligand and metal allows for the insertion of $CO_2$ to form a new M–O bond, leaving the metal's oxidation state unchanged (Scheme 1a).[6] Initial decrease of C–O bond strength upon $CO_2$ insertion into the M–L bond, with concomitant formation of a relatively weak M–O bond, enables functionalization.[6e] To date, a plethora of homogeneous transition-metal catalysts have been developed for thermal, photochemical, and electrochemical conversion of $CO_2$, utilizing this strategy.[1] Additionally, fine-tuning of the ancillary ligand could also promote $CO_2$ insertion and facilitate catalyst regeneration. Therefore, appropriate metal choice, understanding the impact of the ancillary ligand, and additional effects, such as solvent, temperature, *etc.* on $CO_2$ activation is crucial for rational catalyst design. In contrast to transition-metals, a limited number of low valent main-group metal-initiated $CO_2$ activations and catalytic functionalizations have been reported.[3a,4m, 7] Pertinent to this work, insertion of $CO_2$ *via* stanna-amination by (Sn[N(SiMe$_2$R)$_2$]$_2$ (R = Me, Ph) **I**,[4g,h] stanna-borylation by Sn[B(NDippCH)$_2$]$_2$ **II**,[4i] as well as reversible $CO_2$ uptake by P,P-chelated stannylene [(*i*-Pr$_2$P)$_2$N]$_2$Sn **III**,[4j] rendering Sn(II)carboxylates, could be demonstrated (Scheme 1b). Nonetheless, poor stability of these Sn(II)carboxylates

[a] *Dr. D. Sarkar,[+] L. Groll,[+] Dr. F. Hanusch, Prof. S. Inoue*
*Department of Chemistry*
*WACKER-Institute of Silicon Chemistry and Catalysis Research Center*
*Technische Universität München*
*Lichtenbergstraße 4*
*85748 Garching (Germany)*
*E-mail: s.inoue@tum.de*
[b] *Prof. D. Munz*
*Department of Chemistry and Pharmacy*
*General and Inorganic Chemistry*
*Friedrich-Alexander-University Erlangen-Nuremberg (FAU)*
*Egerlandstraße 1*
*91058 Erlangen (Germany)*
*E-mail: dominik.munz@uni-saarland.de*
[c] *Prof. D. Munz*
*Inorganic Chemistry: Coordination Chemistry*
*Saarland University*
*Geb. C4.1*
*66123 Saarbrücken (Germany)*
[+] *These authors contributed equally to this work.*

Supporting information for this article is available on the WWW under https://doi.org/10.1002/cctc.202201048

*Main Group Special Collection*

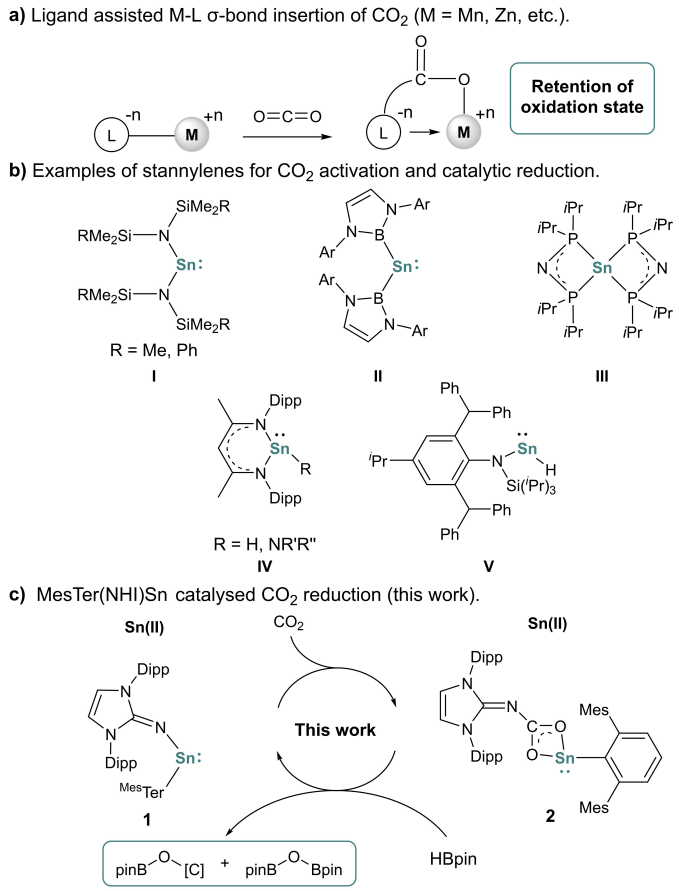


**Scheme 1.** a) Insertion of $CO_2$ by transition metal-ligand bond cleavage. b) Recent examples of stannylenes for $CO_2$ activation and catalytic reduction.[4g–l] c) Two- coordinate stannylene-NHI synergy (Dipp = 2,6-$^{i}Pr_2(C_6H_3)$, Mes = 2,4,6-$Me_3(C_6H_2)$, $^{Mes}$Ter = 2,6-$Mes_2C_6H_3$, pin = pinacolato, R′R″ = $^{i}Pr_2$; R′ = H, R″ = Dipp).

leads to undesired rearrangement reactions, such as diboration of $CO_2$ in case of **II** or the 1,3-shift of a trimethylsilyl group from the ligand to inserted $CO_2$ in case of **I**.[4g–i] This is attributed to the comparatively high oxophilicity of the corresponding ligand functional groups, which impede their catalytic use in $CO_2$ reduction.[4g–j,8]

To the best of our knowledge, merely one example of tetrylene-mediated single-site $CO_2$ activation and catalytic conversion has been reported to date, where the high reactivity of the E(II)–H group facilitates the reduction of $CO_2$ (**V**, Scheme 1b).[4l] However, synergistic activation of $CO_2$ *via* tetrylene-ligand cooperation and subsequent conversion to value added products is not yet reported. Based on these previous accounts, and considering the high electrophilicity of stannylenes, a Sn(II) center connected to an electron-rich and consequently nucleophilic ligand should therefore be an excellent choice to procure $CO_2$ activation and conversion while bypassing the requirement for Sn(II)-Sn(IV) redox shuttling.[4h–k,8a,9] Additionally, the reduced bond strength of Sn(II)–O in comparison to E(II)–O (E = Si, Ge) bonds renders Sn(II) an ideal metal center for $CO_2$ functionalization.[10]

Engineering the Sn-ligand bond, *viz.* polarization or zwitterionic character, may likewise allow to achieve small HOMO-LUMO energy gaps, and thus control of bond activation, elimination, and eventually catalysis.[11] A convenient method to control the polarization of formal multiple bonds is hard-soft mismatch. Recently, we reported *N*-heterocyclic phosphinidene (NHCP)-supported stannylene NHCP=SnAr, which can be regarded as heavier nitrile congener with multiple bonded character between P and Sn.[9b] Moving from the "*N*-heterocyclic phosphinidene (NHCP)" to an *N*-heterocyclic imine (NHI), featuring an electronegative nitrogen atom, should strongly enhance charge separation in the Sn=E bond and consequently facilitate $CO_2$ activation.[12] Due to the readily adjustable steric and electronic properties of NHIs, they are frequently applied in various metalorganic complexes and are an ideal candidate for our purpose.[12a,13]

## Results and Discussion

With this insight in mind, the heteroleptic NHI stannylene **1** $^{Mes}$Ter(NHI)Sn was synthesized *via* treatment of chlorostannylene $^{Mes}$Ter(Cl)Sn with one equivalent of LiN(IDipp), ($^{Mes}$Ter = 2,6-$Mes_2C_6H_3$, NHI = N(IDipp), IDipp = C[N-(2,6-$^{i}Pr_2C_6H_3$)CH]$_2$), (Scheme 2a). Compound **1** was isolated in 75% yield as a dark red solid and is highly soluble in tetrahydrofuran, benzene, or toluene, but poorly soluble in pentane, hexane, or heptane. The $^{119}$Sn{$^{1}$H} NMR spectrum of compound **1** shows a characteristic signal for the tin center at 967.8 ppm, which falls in the range of reported heteroleptic, two-coordinate (aryl)stannylenes ($\delta$ = 197-1919 ppm).[9b,14]

Single crystal X-ray diffraction (SC-XRD) analysis confirmed the structural identity of compound **1**, with the two-coordinate Sn center bound by one NHI and one *m*-terphenyl group (Figure 1). The Sn–N bond length in complex **1** is 2.041(2) Å, which is longer than a Sn–N double bond (1.92 Å) and slightly shorter than a Sn–N single bond of amido-stannylenes (2.08–2.09 Å).[14b,16] The ∠C1–Sn1–N1 bond angle in **1** is 95.62(10)° and is acute in regard to other heteroleptic two coordinate aryl Sn(II) complexes (96.9–117.6°).[9b,14]

To understand the electronic structure of **1**, we performed a computational analysis (PBE0). The HOMO relates to the

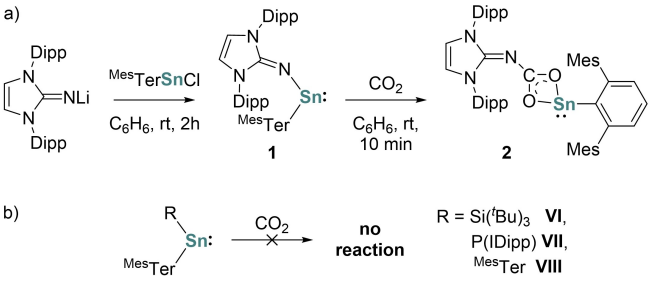


**Scheme 2.** a) Synthesis and reactivity of $^{Mes}$Ter(NHI)Sn, b) Heteroleptic two coordinated (aryl)stannylenes inert towards $CO_2$ (IDipp = C[N-(2,6-$^{i}Pr_2C_6H_3$)CH]$_2$, Dipp = 2,6-$^{i}Pr_2(C_6H_3)$, Mes = 2,4,6-$Me_3(C_6H_2)$, $^{Mes}$Ter = 2,6-$Mes_2C_6H_3$).[9b,14a, 15]

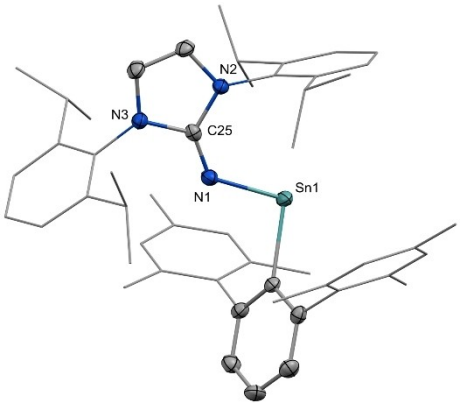


**Figure 1.** Molecular structure of compound **1** in the solid state. Ellipsoids are set at the 50% probability level; hydrogen atoms are omitted for clarity. Selected bond lengths [Å] and bond angles [°]: Sn1–N1 2.041(2), Sn1–C1 2.232(3), N1–Sn1–C1 95.62(10).

stannylene's lone pair, whereas the LUMO is associated with the Sn–N antibonding π-type orbital, which features strong Sn($p_z$) character. The two frontier orbitals are separated by 3.83 eV ($E^{s/t} = 241$ kJ mol$^{-1}$; Figure 2), which is larger than in **VI** ($^{Mes}$Ter(Si$^t$Bu$_3$)Sn, 3.08 eV) yet in the same order of magnitude as found in **VII** ($^{Mes}$Ter[P(IDipp)]Sn, 3.88 eV).[9b,14a] However, the Sn–N bonding in **1** differs distinctly from Sn–P bonding in **VII** (Figure S21). In **1**, the HOMO-2 relates to the lone pair at the NHI, which profits from delocalization within the π-system of the imidazoline substituent, thus leading to a weak Sn–N π-interaction. In contrast, the HOMO-1 of **VII** demonstrates a genuine Sn–P π-bond.[9b] Accordingly, Mayer's Bond Order and Löwdin's partial charge analysis corroborate the strongly polarized nature of the Sn$^{\delta+}$–N$^{\delta-}$ single bond (Mayer Bond Order, Sn–N: 1.1; Löwdin's Partial Charges, Sn: +0.4 a.u., N: −0.4 a.u.), whereas the Sn–P bond is rather multiple-covalent in **VII** (Sn=P: 1.6; Sn: +0.2 a.u., P: +0.2 a.u.). In case of **3** (*vide infra*), the electronic structure changes, and the HOMO (-5.41 eV) represents the amine's lone pair, which is delocalized within the aryl substituents, while the HOMO-1 relates to the Sn lone pair (−6.11 eV).

Motivated by our interest in small molecule activation, we were enticed to determine, whether compound **1** shows reactivity towards $CO_2$. A trial NMR scale reaction of **1** with $CO_2$ (1 bar) at room temperature in $C_6D_6$ afforded a color change from red to colorless within 10 min. Heteronuclear NMR analysis confirmed the quantitative conversion of **1** to a tin-carboxylate complex **2**. The $^{119}$Sn{$^1$H} NMR spectrum revealed resonances for a distinct $^{119}$Sn nucleus at 323.3 ppm, which resonates in the up-field region compared to **1** and literature reported tin-carbamate complex (δ = +393 ppm).[8a] Further, in the $^{13}$C NMR of **2**, a characteristic signal was observed at 175.6 ppm, which is indicative of a carbamate carbon. Compound **2** evolved thermodynamically stable and did not convert back to **1**, neither at elevated temperatures nor under reduced pressure. [$^{Mes}$TerSn($CO_2$)N(IDipp)] was therefore isolated on a preparative scale as a colorless solid in 96% yield. SC-XRD of **2** confirmed the insertion of $CO_2$ into the Sn–NHI bond, yielding a tetrahedral tin center, κ$^2$*O,O′* coordinated by the carbamato group (Figure 3, Sn1–O1 2.2066(12), Sn1–O2 2.1971(12)).

This facile access to a tin-carbamate complex directly from $CO_2$ presents an attractive entry to carbon dioxide valorization.[4i,j, 8a] Notably, $^{Mes}$Ter(Si$^t$Bu$_3$)Sn **VI** (3.08 eV) and $^{Mes}$Ter($^{Mes}$Ter)Sn **VIII** (3.51 eV) are not able to activate $CO_2$, despite their lower HOMO-LUMO gaps (Scheme 2b). Also **VII**, which 1,2 adds ketenes and catalytically reduces aldehydes and ketones, does not react with $CO_2$.[9b]

The mechanisms for the $CO_2$ activation by **1** and **VII** were calculated (DLPNO-CCSD(T)/def2-TZVPP//PBE0-D3/def2-SVP) including correction for solvation in benzene. The computations reveal that two mechanisms are feasible in case of **1** (Scheme 3). The transition state, which is higher in energy ($\Delta G^{\ddagger} = +81$ kJ mol$^{-1}$), is to be understood as nucleophilic attack of the *N*-heterocyclic imine at carbon dioxide. Note that the comparatively higher barrier is consistent with the HOMO being located at tin, whereas the NHI lone pair is the HOMO-2. The other,

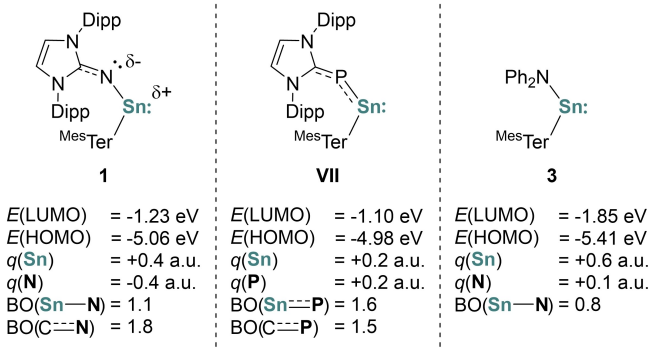


**Figure 2.** Frontier orbital energies and population analysis (Löwdin charges, Mayer Bond Order, PBE0/def-TZVPP//PBE0-D3/def2-SVP) of **1** and comparison with **VII** and **3**. (Dipp = 2,6-$^i$Pr$_2$($C_6H_3$), Mes = 2,4,6-Me$_3$($C_6H_2$), $^{Mes}$Ter = 2,6-Mes$_2$$C_6H_3$).

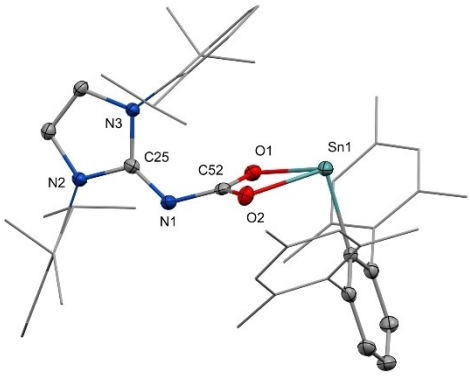


**Figure 3.** Molecular structures of compound **2** in the solid state. Ellipsoids are set at the 50% probability level; hydrogen atoms are omitted for clarity. Selected bond lengths [Å] and bond angles [°]: Sn1–O1 2.2066(12), Sn1–O2 2.1971(12), O1–C52 1.2842(19), O2–C52 1.2787(19), N1–C52 1.360(2), N1–C25 1.300(2), N2–C25 1.3729(19), N3–C25 1.3721(19), O1–Sn1–O2 59.71(4).

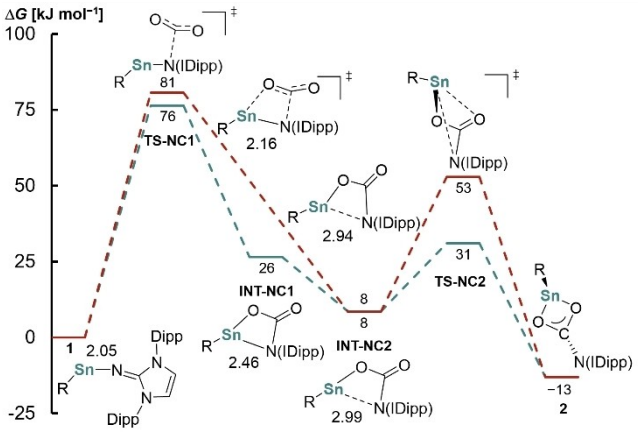


**Scheme 3.** Computed mechanism for the $CO_2$ activation by **1**. (R = $^{Mes}$Ter, $^{Mes}$Ter = 2,6-$Mes_2C_6H_3$, Mes = 2,4,6-$Me_3(C_6H_2)$, Dipp = 2,6-$^{i}Pr_2(C_6H_3)$, IDipp = C-[N-(2,6-$^{i}Pr_2C_6H_3$)CH]$_2$.

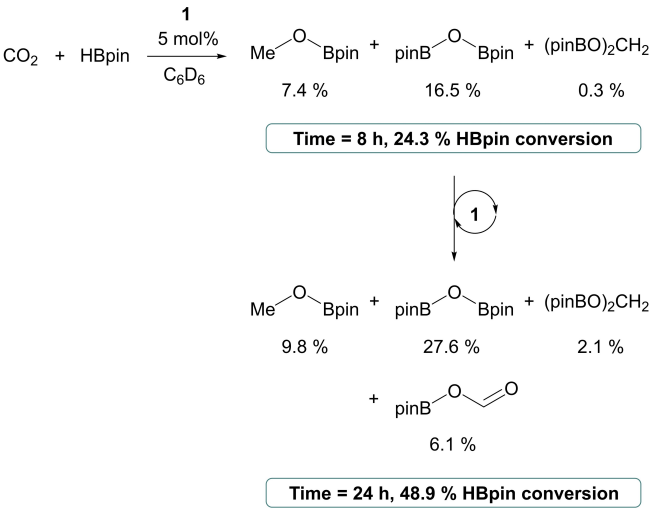


**Scheme 4.** Hydroboration products obtained from the reaction of HBpin with $CO_2$ (1 bar) with **1** (5 mol%) as catalyst at 25 °C (in $C_6D_6$). Overall HBpin conversion based on $^{11}$B NMR integrals, ratio of products based on $^{1}$H NMR integrals relative to 0.33 eq. of 1,3,5-trimethoxybenzene as internal standard.

more favorable transition state relates to the 1,2-addition across the strongly polarized π-system of the Sn–N moiety (**TS-NC1**, $\Delta G^{\ddagger} = +76$ kJ mol$^{-1}$). This latter mechanism affords first intermediate **INT-NC1** ($\Delta G = +26$ kJ mol$^{-1}$), where a Sn–N bond is still present. Barrierless dissociation gives **INT-NC2** ($\Delta G = +8$ kJ mol$^{-1}$), which affords the $\mu^3$-coordinate adduct **2** ($\Delta G = -13$ kJ mol$^{-1}$) *via* **TS-NC2** ($\Delta G^{\ddagger} = +31$ kJ mol$^{-1}$).

In case of the phosphorus congener, where the phosphorus atom lacks distinct nucleophilic properties, the activation proceeds through the 1,2-addition mechanism only (*cf.* Scheme S1). The activation of $CO_2$ is predicted to be facile with $\Delta G^{\ddagger} = +84$ kJ mol$^{-1}$ for **TS-PC1**. However, the transition state **TS-PC2**, which breaks the Sn–P bond, is high in energy ($\Delta G^{\ddagger} = +128$ kJ mol$^{-1}$). Accordingly, Sn–P bond cleavage to give **PC2**, which is the P-congener of **2**, proceeds overall endergonic ($\Delta G = +39$ kJ mol$^{-1}$). We thus conclude that enhanced covalency in the phosphorus-tin compound **VII** thermodynamically disfavors $CO_2$ activation, whereas hard-soft mismatch (orbital-energy mismatch, respectively) facilitates bond activation through strong polarization of the Sn–N bond in **1**.

Consequently, we were interested, if **1** would be applicable for the hydroboration of $CO_2$ using HBpin (pin = pinacolato) as reductant. As anticipated, treating **2** with equimolar amounts of HBpin in $C_6D_6$ at room temperature led to the formation of MeOBpin (9%) and pinBOBpin (5%) after 30 minutes. Additionally, in this mixture a new septet was observed at 3.19 ppm (*cf.* Figure S14), which possibly stems from an unidentified active catalyst species. Despite several attempts, isolation of this active catalyst from the reaction mixture was unsuccessful. However, alternating addition of 1 bar of $CO_2$ and one equivalent of HBpin to this reaction mixture clearly shows the increasing formation of MeOBpin (31% yield after three alternating additions). This observation implies, that **1** could also act as a precatalyst. Indeed, 5 mol% of **1** catalytically converts $CO_2$ to MeOBpin, pinBOBpin, $(pinBO)_2CH_2$ and pinBO(C=O)H (Scheme 4).

Solvent optimization studies revealed a moderately higher reaction rate in polar (*e.g.*, rt, THF-$d_8$, *TOF* = 1.8 h$^{-1}$) than in non-polar solvents (*e.g.*, rt, $C_6D_6$, *TOF* = 1.2 h$^{-1}$). With the above points in mind and after temperature optimization, we found that using 5 mol% of **1** with HBpin in THF at 50 °C provides the optimal reaction conditions for complete conversion of HBpin to MeOBpin, and pinBOBpin (*TOF* = 4.2 h$^{-1}$, 1 bar $CO_2$). The longevity of the catalyst could be demonstrated by repeating the reaction multiple times, where gradual decrease of the catalytic activity was observed (*e.g.*, 50 °C, THF-$d_8$ *TOF*(Run 1) = 4.2 h$^{-1}$ vs. *TOF*(Run 4) = 2.9 h$^{-1}$). After the seventh run, no catalytic conversion was observed and the formation of black precipitate at the bottom of the NMR tube indicated decomposition of the catalyst into metallic tin. To rule out hidden boron catalysis by *in situ* formed $BH_3$ ($BH_4^-$, respectively) and to assess the stability of **1**, we conducted a stoichiometric reaction of **1** with HBpin in absence of $CO_2$.[17] Here, no reaction between the complex and the reductant, as well as no formation of aforementioned boranes, could be observed. Additionally, a control experiment with the free NHI ligand HN(IDipp) (5 mol% HN(IDipp), 1 eq. HBpin, 1 bar $CO_2$, in $C_6D_6$ at 25 °C) was performed, which showed no notable conversion of HBpin after eight hours.

To elucidate the mechanism for $CO_2$ reduction, further computations were conducted. Especially the hydrogenation step proved intriguing. The computations for two isomers corroborate that the direct borylation of the $CO_2$ group by HBpin is indeed facile (Scheme S3, **TS-BH1**, $\Delta G^{\ddagger} = +59$ kJ mol$^{-1}$). In contrast, the hydride transfer from the borohydride to the central carbon atom of the $CO_2$ group (Scheme S3, **TS-BH2**) is associated with a high activation energy of at least $\Delta G^{\ddagger} = +132$ kJ mol$^{-1}$. These values are hardly consistent with an experimental reaction temperature of 50 °C, which relates to a barrier around $\Delta G^{\ddagger} = +100$ kJ mol$^{-1}$, even

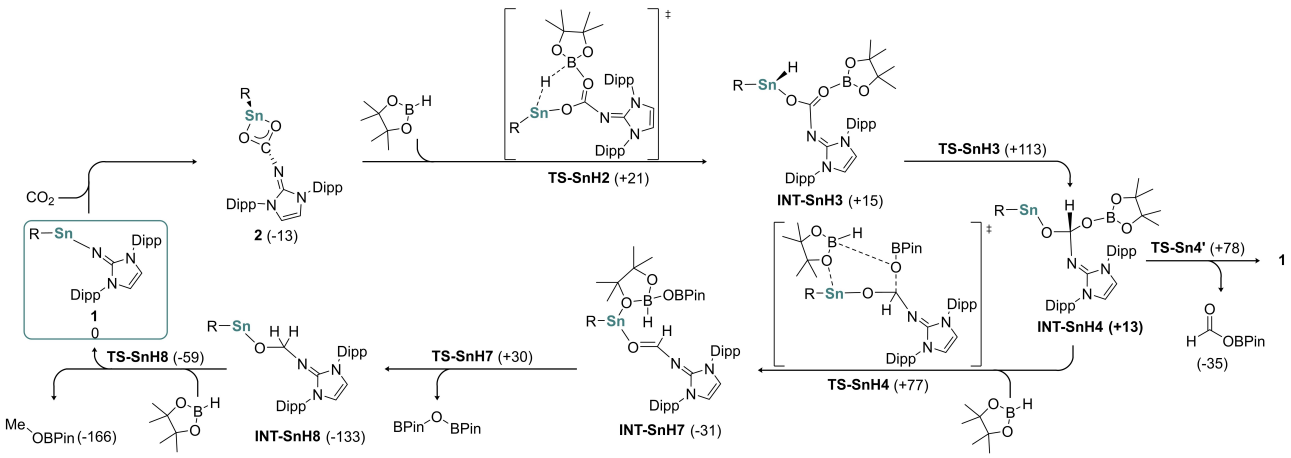


**Scheme 5.** Proposed mechanism of $^{Mes}$Ter[N(IDipp)]Sn catalyzed hydroboration of $CO_2$. ΔG (kJ mol$^{-1}$) values are given in parentheses. (R = $^{Mes}$Ter = 2,6-Mes$_2$C$_6$H$_3$, Dipp = 2,6-$^i$Pr$_2$(C$_6$H$_3$), Mes = 2,4,6-Me$_3$(C$_6$H$_2$), $^{Mes}$Ter = 2,6-Mes$_2$C$_6$H$_3$, pin = pinacolato). See Schemes S3, S4, S6 for more details including intermediates, which have been omitted for clarity.

more so if considering that **2** (*cf.* Scheme 3, $\Delta G = -13$ kJ mol$^{-1}$) is the resting state of the catalytic cycle. However, forming the stanna-hydride **INT-SnH3** is very facile (Scheme 5, $\Delta G^{\ddagger} = +21$ kJ mol$^{-1}$, $\Delta G = +15$ kJ mol$^{-1}$). Also, the subsequent migration of the hydride to give the formyl derivative **INT-SnH4**, is predicted to occur under comparatively mild conditions ($\Delta G^{\ddagger} = +113$ kJ mol$^{-1}$, $\Delta G = +13$ kJ mol$^{-1}$). These values are in much better agreement with the experimental conditions.

The release of the reduced products through hydrogenation by HBpin proceeds with lower barriers as was found for the previous step, which thus represents the rate-determining transition state of the overall catalytic cycle. A second borylation step (**TS-SnH4**, $\Delta G^{\ddagger} = +77$ kJ mol$^{-1}$) may give **INT-SnH7**, ($\Delta G = -31$ kJ mol$^{-1}$). Subsequent hydride transfer *via* **TS-SnH7** ($\Delta G^{\ddagger} = +30$ kJ mol$^{-1}$) affords **INT-SnH8** ($\Delta G = -133$ kJ mol$^{-1}$), which may reversibly eliminate ($\Delta G = -127$ kJ mol$^{-1}$) formaldehyde (Scheme S5; **TS-Sn8**, $\Delta G^{\ddagger} = -59$ kJ mol$^{-1}$), thereby regenerating **1**. Analogously, H-(CO)OBpin may be released reversibly from a conformer of **INT-SnH4** (Scheme S5; **TS-Sn4'**, $\Delta G^{\ddagger} = +78$ kJ mol$^{-1}$; $\Delta G = -35$ kJ mol$^{-1}$), whereas borylation of, for instance, **INT-SnH8** will eventually lead to the formation of MeOBPin ($\Delta G = -166$ kJ mol$^{-1}$).

In order to highlight the relevance of the NHI ligand in the catalytic $CO_2$ reduction with **1**, we synthesized $^{Mes}$Ter(NPh$_2$)Sn **3** with a similarly low oxophilic –NPh$_2$ group replacing the NHI moiety.[4g–j,8a] **3** was obtained *via* the reaction of $^{Mes}$Ter(Cl)Sn with LiNPh$_2$ (Scheme 6) and characterized by single-crystal XRD and standard NMR techniques (*cf.* SI). Treatment of **3** with 1 bar $CO_2$ in C$_6$D$_6$ leads to a gradual color change from deep red to yellow in about 10 minutes. According to $^1$H and $^{13}$C NMR, as well as mass spectrometry (*cf.* SI), the formation of a new compound, which we hypothesize to be a $CO_2$ adduct of **3**, presumably a tin-carboxylate, is observed. In agreement, the computational analysis indicates that the insertion of $CO_2$ into **3** should be exergonic by $-27$ kJ mol$^{-1}$ (Scheme S2). However, the compound could not be isolated and the characterization

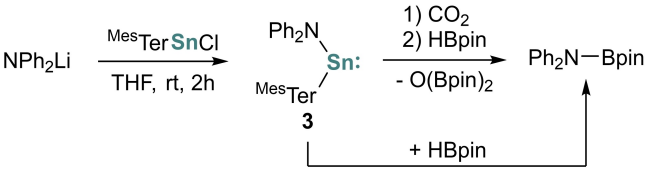


**Scheme 6.** Synthesis and reactivity of $^{Mes}$Ter(NPh$_2$)Sn with $CO_2$ and HBpin. (Mes = 2,4,6-Me$_3$(C$_6$H$_2$), $^{Mes}$Ter = 2,6-Mes$_2$C$_6$H$_3$, pin = pinacolato).

by $^{119}$Sn{$^1$H} NMR spectroscopy was unsuccessful. Upon addition of equimolar amounts of HBpin to the mixture, the formation of amineborane Ph$_2$N-Bpin and pinBOBpin was observed, rendering the regeneration of **3** unsuccessful (Scheme 6). Unlike the conversion of $CO_2$ with NHI stabilized stannylene **1**, no other products indicative of a hydroboration reaction, were found. Similarly, **3** is unstable in the presence of HBpin, leading to the formation of aforementioned amineborane, protonated ligand, and deposition of elemental tin.

This outcome is in good agreement with the computational analysis of the electronic structure of **3** (*cf.* Figure 2). Indeed, and as expected due to the small HOMO-LUMO energy gap of only 3.56 eV and the polarized character of the Sn–N bond (Sn: +0.6 a.u., N: +0.1 a.u.), **3** activates $CO_2$ readily. However, the low bond order indicates a weaker Sn–N bond and a more nucleophilic amide, rendering it susceptible to the irreversible and undesired reaction with HBpin. Thus, this study signifies the importance of the unique donor abilities of the NHI, enabling stabilization of tin-carboxylate complex **2** as well as regeneration of **1** in this stannylene-mediated $CO_2$ reduction.

## Conclusion

In summary, the ligand assisted activation and catalytic reduction of $CO_2$ to commodity chemicals by an NHI-stabilized stannylene is reported for the first time. Both experimental and

computational investigations revealed the effectiveness of the tunable Sn/NHI interaction, involving Sn/NHI dissociation and the intermediate formation of tin hydrides. Thus, our design protocol to translate the concept of ligand assisted transition-metal ligand σ-bond cleavage to main group chemistry indicates a promising avenue towards the cooperativity between a heavy p-block element and a ligand.

## Experimental Section

### General Information

All experiments and manipulations were carried out under a dry argon atmosphere using standard *Schlenk* techniques or a glovebox. All glass junctions were coated with PTFE-based grease *Merkel* Triboflon III. N-hexane, n-pentane, THF, benzene and toluene were refluxed over sodium/benzophenone, freshly distilled and deoxygenated prior to use. The $^{1}H$, $^{13}C$, and $^{119}Sn$ NMR spectra were measured on *Bruker* 400 MHz and 500 MHz spectrometers. Chemical shifts were referenced to residual solvent signals ($^{1}H$ and $^{13}C$ NMR). $^{119}Sn$ NMR chemical shifts were referenced to $Me_4Sn$ ($^{119}Sn$). Deuterated solvent $C_6D_6$ and THF-$d_8$ were obtained from *Deutero* Deutschland GmbH and were dried over 4 Å molecular sieves prior to use. Unless otherwise stated, all reagents were purchased from commercial sources and used as received. Elemental analyses (EA) were conducted with a EURO EA (*HEKA tech*) instrument equipped with a CHNS combustion analyzer. Thereby, all samples were prepared in THF solutions, filtered and injected into the spectrometers. TOF analyzation in cationic mode resulted in the obtained spectra (see SI), which were resolved by mass-to-charge values. Liquid Injection Field Desorption Ionization Mass Spectrometry (LIFDI-MS) was performed in an inert atmosphere glovebox with a *Thermo Fisher* Scientific Exactive Plus Orbitrap equipped with an ion source from Linden CMS.S7.[18] NHILi, [$^{Mes}$TerSnCl] and $Ph_2NLi$ were synthesized according to literature procedures.[15a,19]

### $^{Mes}$Ter[N(IDipp)]Sn (1)

A benzene (5 mL) solution of NHILi (0.5 g, 1.22 mmol, 1.00 eq) was added to $^{Mes}$TerSnCl (0.57 g, 1.22 mmol, 1.00 eq) in benzene (3 mL) at room temperature. The color of the solution rapidly changed from orange to dark red. After stirring the solution for 2 h, the solvent was removed *in vacuo*. The obtained residue was washed with pentane (3×2 mL), extracted with a mixture of toluene (10 mL) + hexane (2 mL) and filtered through a microfiber glass filter. The solution was concentrated to approximately 2 mL and placed at −25 °C and after two weeks compound **1** was obtained as an analytically pure red crystalline material (0.77 g, 0.54 mmol, 75 %). **$^{1}$H NMR** (400.13 MHz, 298 K, $C_6D_6$): δ = 1.09, 1.11, 1.14 (m, 24H, CH($CH_3$)$_2$, NHI), 2.08 (s, 12H, 4×$C^{2,6}$-$CH_3$, Mes), 2.29 (s, 6H, 2x$C^4$-$CH_3$, Mes), 3.06 (hept, $^{3}J_{H-H}$ = 6.7 Hz, 4H, CH($CH_3$)$_2$), 5.94 (s, 2H, N-CH), 6.65 (s, 4H, 2×$C^{3,5}$-H, Mes), 6.85, 6.88 (2H, $C^{3,5}$-$C_6H_3$), 7.04-7.06 (4H, 2×$C^{3,5}$-H, Dipp, NHI), 7.16-7.23 (3H, $C^4$-$C_6H_3$, 2×$C^4$-H, Dipp) ppm. **$^{13}$C{$^{1}$H} NMR** (125.83 MHz, 298 K, $C_6D_6$): δ = 21.6–21.9 ($C^{2,4,6}$-$CH_3$, Mes), 23.4 (CH($CH_3$)$_2$), 24.9 (CH($CH_3$)$_2$), 29.2 (CH($CH_3$)$_2$), 114.8 (N-CH-, NHI), 124.3-148.1 (Ar-C, Mes, NHI), 155.8 (NCN) ppm. **$^{119}$Sn{$^{1}$H} NMR** (149.20 MHz, 298 K, THF-$d_8$): 967.8 ppm. **Anal. Calcd. [%] for $C_{51}H_{61}N_3Sn$**: C, 73.38; H, 7.37; N, 5.03. Found C, 73.12; H, 7.21; N, 4.89.

### [$^{Mes}$TerSn($CO_2$)N(IDipp)] (2)

The benzene (2 mL) solution of **1** (100 mg, 0.11 mmol, 1.00 eq) in a Schlenk flask was freeze-pump-thaw degassed two times before being refilled with 1 bar of $CO_2$. After refilling with $CO_2$, the red solution immediately turned colorless. The solution was stirred for 15 minutes, followed by the removal of all volatiles. The resulting solid was dissolved in a mixture of THF (2 mL) and n-hexane (2 mL) and placed at −35 °C for eight days, which yielded colorless crystals of compound **2** (102 mg, 0.12 mmol, 97 %). **$^{1}$H NMR** (400.13 MHz, 298 K, $C_6D_6$): δ = 1.09–1.31 (m, 24H, CH($CH_3$)$_2$, NHI), 2.12 (s, 12H, 4×$C^{2,6}$-$CH_3$, Mes), 2.30 (s, 6H, 2×$C^4$-$CH_3$, Mes), 2.92 (hept, $^{3}J_{H-H}$ = 6.7 Hz, 4H, CH($CH_3$)$_2$), 5.90 (s, 2H, N-CH), 6.86 (s, 4H, 2×$C^{3,5}$-H, Mes), 6.98-7.03 {6H, (2H, $C^{3,5}$-$C_6H_3$), (4H, 2×$C^{3,5}$-H, Dipp, NHI)}, 7.10–7.21 {3H, $C^4$-$C_6H_3$, (2×$C^4$-H, Dipp)} ppm. **$^{13}$C{$^{1}$H} NMR** (125.83 MHz, 298 K, $C_6D_6$): δ = 21.3–21.5 ($C^{2,4,6}$-$CH_3$, Mes), 23.6 (CH($CH_3$)$_2$), 24.7 (CH($CH_3$)$_2$), 29.1 (CH($CH_3$)$_2$), 115.9 (N-CH-, NHI), 124.2-147.6 (Ar-C, Mes, NHI), 169.9 (NCN), 175.6 (OCO) ppm. **$^{119}$Sn{$^{1}$H} NMR** (149.20 MHz, 298 K, $C_6D_6$): 323.1 ppm. **Anal. Calcd. [%] for $C_{52}H_{61}N_3O_2Sn$**: C, 71.07; H, 7.00; N, 4.78. Found C, 70.88; H, 6.81; N, 4.71.

### $^{Mes}$Ter($NPh_2$)Sn (3)

$^{Mes}$TerSnCl (100 mg, 0.21 mmol, 1.00 eq.) and $Ph_2NLi$ (37.46 mg, 0.21 mmol, 1.00 eq.) were each dissolved in THF (5 ml) respectively. The $Ph_2NLi$ solution was then added dropwise to the $^{Mes}$TerSnCl solution at room temperature while stirring, giving an orange mixture. The mixture was then stirred for another 60 minutes. Subsequently, the volatiles were removed *in vacuo* and the red residue was extracted with $Et_2O$ (2×3 mL) and filtered through a microfiber glass filter. After once more drying *in vacuo*, the raw product was recrystallized in a minimal amount of pentane at −35 °C, resulting in the formation of dark red crystals of compound **3** (65.5 mg, 0.11 mmol, 51 %). **$^{1}$H NMR** (400.13 MHz, 298 K, $C_6D_6$): δ = 2.15 (s, 12H, 4x$C^{2,6}$-$CH_3$), 2.17 (s, 6H, 2x$C^4$-$CH_3$, Mes), 6.48 (d, $^{3}J_{H-H}$ = 7.7 Hz, 4H, 2x$C^{2,6}$-H, Ph), 6.88-6.79 (m, 6H, 2x$C^{3,5}$-H, Mes, 2x$C^{}$, Ph), 7.06-6.95 (m, 6H, 2x$C^{3,5}$-H, Ph, $C^{3,5}$-H, Ter), 7.23 (t, $^{3}J_{H-H}$ = 7.5 Hz, 1H, $C^4$-H, Ter) ppm. **$^{13}$C{$^{1}$H} NMR** (75 MHz, 298 K, $C_6D_6$): δ = 21.14–21.55 ($C^{2,4,6}$-$CH_3$, Mes), 118.24-129.55 (Ar-C, $^{Mes}$Ter, Ph), 135.79 (Sn-C), 153.82 (N-C) ppm. **$^{119}$Sn{$^{1}$H} NMR** (149.20 MHz, 298 K, $C_6D_6$): 903.81 ppm. **LIFDI-MS Calcd. for $C_{36}H_{35}NSn$**: 601.17914 Found: 601.17546. **Anal. Calcd. [%] for $C_{36}H_{35}NSn$**: C, 72.02; H, 5.88; N, 2.33; Sn, 19.77. Found: C, 68.56; H, 5.88; N, 2.29; Sn, 19.70. (N.B. Despite several attempts, elemental analysis showed consistently low C values with simultaneously excellent agreement of H and N values, presumably due to formation of incombustible material).

### Adduct-formation upon Reaction of 3 with $CO_2$

$^{Mes}$Ter($NPh_2$)Sn (20 mg, 0.07 mmol; 1.00 eq.) was dissolved in 0.5 mL benzene in a Schlenk flask and freeze-pump-thaw degassed two times. Subsequently, the flask was refilled with 1 bar of $CO_2$, resulting in a color change from deep red to yellow in the span of about 10 minutes. The reaction was quantitative according to NMR spectroscopy, however the product could not be isolated in solid state. **$^{1}$H NMR** (400.13 MHz, 298 K, $C_6D_6$): δ = 2.17 (s, 12H, 4x$C^{2,6}$-$CH_3$, Mes), 2.27 (s, 6H, 2×$C^4$-$CH_3$, Mes), 6.84 (s, 4H, 2×$C^{3,5}$-H, Mes), 7.01 (d, $^{3}J_{H-H}$ = 7.5 Hz, 2H, $C^{3,5}$-H, Ter), 7.08–7.15 (m, 10H, Ar-H, Ph), 7.25 (t, $^{3}J_{H-H}$ = 7.5 Hz, 1H, $C^4$-H, Ter) **$^{13}$C{$^{1}$H} NMR** (101 MHz, 298 K, $C_6D_6$): δ = 21.41 ($C^4$-$CH_3$, Mes), 21.68 ($C^{2,6}$-$CH_3$, Mes), 124.35–128.96 (Ar-CH, Mes, Ph), 136.37 (Ar-CH, Mes), 138.83 ($C^{3,5}$-CH, Ter) 142.90 (Ar-C, Ph), 147.98 ($C^4$-CH, Ter), 160.81 (OCO) ppm. **LIFDI-MS Calcd. for $C_{37}H_{36}NO_2Sn$**: 645.16897 Found: 645.16863.

**Catalytic Hydroboration of $CO_2$ by 1**

All catalytic reactions were performed according to the following procedure in either $C_6D_6$ at room temperature, or in THF-$d_8$ at room temperature or 50 °C respectively. 2.9 mg of $^{Mes}$Ter[N(IDipp)]Sn (0.003 mmol, 0.05 eq.) were dissolved in 0.4 ml of the respective deuterated solvent in a *J-young* NMR tube. Then, 10 µl of HBpin (8.82 mg, 0.063 mmol, 1.0 eq.) and 0.046 ml of a 0.5 M solution of 1,3,5-methoxybenzene in $C_6D_6$ (0.023 mmol, 0.33 eq.) were added. The NMR tube was freeze-pump-thaw degassed two times before being refilled with 1 bar of $CO_2$. The reactions at room temperature were terminated after 24 h, the reaction at 50 °C after 6 h. Time course data of product yields and overall conversion were determined by $^1$H- and $^{11}$B-NMR data.

## *Acknowledgements*

*We gratefully acknowledge financial support from the Deutsche Forschungsgemeinschaft (In 234/7-1), and DAAD (fellowship for D.S.). D.M. thanks the RRZ Erlangen for computational resources and the Fonds der chemischen Industrie im Verband der chemischen Industrie e.V. for a Liebig fellowship. We are also thankful for M. Muhr for providing Mass Spectrometric data. Open Access funding enabled and organized by Projekt DEAL.*

## *Conflict of Interest*

The authors declare no conflict of interest.

## Data Availability Statement

The data that support the findings of this study are available in the supplementary material of this article.

**Keywords:** Tin · Small Molecule Activation · $CO_2$ Activation · Stannylene · Tetrylenes

[1] a) Q. Liu, L. Wu, R. Jackstell, M. Beller, *Nat. Commun.* **2015**, *6*, 5933; b) C. Maeda, Y. Miyazaki, T. Ema, *Catal. Sci. Technol.* **2014**, *4*, 1482–1497; c) C. C. Chong, R. Kinjo, *ACS Catal.* **2015**, *5*, 3238–3259; d) M. Cokoja, C. Bruckmeier, B. Rieger, W. A. Herrmann, F. E. Kühn, *Angew. Chem. Int. Ed.* **2011**, *50*, 8510–8537; *Angew. Chem.* **2011**, *123*, 8662–8690; e) W.-H. Wang, Y. Himeda, J. T. Muckerman, G. F. Manbeck, E. Fujita, *Chem. Rev.* **2015**, *115*, 12936–12973.

[2] a) S. Kostera, M. Peruzzini, L. Gonsalvi, *Catalysts* **2021**, *11*, 58; b) X. Yin, J. R. Moss, *Coord. Chem. Rev.* **1999**, *181*, 27–59; c) C. Weetman, S. Inoue, *ChemCatChem* **2018**, *10*, 4213–4228; d) T. Biswal, K. P. Shadangi, P. K. Sarangi, R. K. Srivastava, *Chemosphere* **2022**, *298*, 134299; e) K. A. Grice, *Coord. Chem. Rev.* **2017**, *336*, 78–95; f) S. P, S. K. Mandal, *Chem. Sci.* **2020**, *11*, 10571–10593; g) K. Kuciński, G. Hreczycho, *Green Chem.* **2020**, *22*, 5210–5224.

[3] a) S. Yadav, S. Saha, S. S. Sen, *ChemCatChem* **2016**, *8*, 486–501; b) S. Fujimori, S. Inoue, *Eur. J. Inorg. Chem.* **2020**, 3131–3142; c) F. Hanusch, L. Groll, S. Inoue, *Chem. Sci.* **2021**, *12*, 2001–2015.

[4] a) D. Wendel, A. Porzelt, F. A. D. Herz, D. Sarkar, C. Jandl, S. Inoue, B. Rieger, *J. Am. Chem. Soc.* **2017**, *139*, 8134–8137; b) A. V. Protchenko, P. Vasko, D. C. H. Do, J. Hicks, M. Á. Fuentes, C. Jones, S. Aldridge, *Angew. Chem. Int. Ed.* **2019**, *58*, 1808–1812; *Angew. Chem.* **2019**, *131*, 1822–1826; c) D. Reiter, P. Frisch, D. Wendel, F. M. Hörmann, S. Inoue, *Dalton Trans.* **2020**, *49*, 7060–7068; d) A. Jana, D. Ghoshal, H. W. Roesky, I. Objartel, G. Schwab, D. Stalke, *J. Am. Chem. Soc.* **2009**, *131*, 1288–1293; e) A. Jana, G. Tavčar, H. W. Roesky, M. John, *Dalton Trans.* **2010**, *39*, 9487–9489; f) G. Tan, W. Wang, B. Blom, M. Driess, *Dalton Trans.* **2014**, *43*, 6006–6011; g) L. R. Sita, J. R. Babcock, R. Xi, *J. Am. Chem. Soc.* **1996**, *118*, 10912–10913; h) J. R. Babcock, L. Liable-Sands, A. L. Rheingold, L. R. Sita, *Organometallics* **1999**, *18*, 4437–4441; i) A. V. Protchenko, M. Á. Fuentes, J. Hicks, C. McManus, R. Tirfoin, S. Aldridge, *Dalton Trans.* **2021**, 9059–9067; j) D. A. Dickie, E. N. Coker, R. A. Kemp, *Inorg. Chem.* **2011**, *50*, 11288–11290; k) A. Jana, H. W. Roesky, C. Schulzke, A. Döring, *Angew. Chem. Int. Ed.* **2009**, *48*, 1106–1109; *Angew. Chem.* **2009**, *121*, 1126–1129; l) T. J. Hadlington, C. E. Kefalidis, L. Maron, C. Jones, *ACS Catal.* **2017**, *7*, 1853–1859; m) C. Shan, S. Yao, M. Driess, *Chem. Soc. Rev.* **2020**, *49*, 6733–6754.

[5] a) T. Chu, G. I. Nikonov, *Chem. Rev.* **2018**, *118*, 3608–3680; b) P. P. Power, *Nature* **2010**, *463*, 171–177.

[6] a) C. Erken, A. Kaithal, S. Sen, T. Weyhermüller, M. Hölscher, C. Werlé, W. Leitner, *Nat. Commun.* **2018**, *9*, 4521; b) A. Kumar, P. Daw, N. A. Espinosa-Jalapa, G. Leitus, L. J. W. Shimon, Y. Ben-David, D. Milstein, *Dalton Trans.* **2019**, *48*, 14580–14584; c) S. P. Cronin, J. M. Strain, M. S. Mashuta, J. M. Spurgeon, R. M. Buchanan, C. A. Grapperhaus, *Inorg. Chem.* **2020**, *59*, 4835–4841; d) S. Chakraborty, O. Blacque, H. Berke, *Dalton Trans.* **2015**, *44*, 6560–6570; e) N. Hazari, J. E. Heimann, *Inorg. Chem.* **2017**, *56*, 13655–13678.

[7] a) X. Wang, C. Xia, L. Wu, *Green Chem.* **2018**, *20*, 5415–5426; b) N. von Wolff, G. Lefèvre, J. C. Berthet, P. Thuéry, T. Cantat, *ACS Catal.* **2016**, *6*, 4526–4535; c) B.-X. Leong, J. Lee, Y. Li, M.-C. Yang, C.-K. Siu, M.-D. Su, C.-W. So, *J. Am. Chem. Soc.* **2019**, *141*, 17629–17636.

[8] a) L. A. M. Harris, M. P. Coles, J. R. Fulton, *Inorg. Chim. Acta* **2011**, *369*, 97–102; b) K. P. Kepp, *Inorg. Chem.* **2016**, *55*, 9461–9470.

[9] a) S. Weiß, M. Widemann, K. Eichele, H. Schubert, L. Wesemann, *Dalton Trans.* **2021**, *50*, 4952–4958; b) V. Nesterov, R. Baierl, F. Hanusch, A. E. Ferao, S. Inoue, *J. Am. Chem. Soc.* **2019**, *141*, 14576–14580; c) T. J. Hadlington, M. Hermann, G. Frenking, C. Jones, *J. Am. Chem. Soc.* **2014**, *136*, 3028–3031; d) A. V. Protchenko, J. I. Bates, L. M. A. Saleh, M. P. Blake, A. D. Schwarz, E. L. Kolychev, A. L. Thompson, C. Jones, P. Mountford, S. Aldridge, *J. Am. Chem. Soc.* **2016**, *138*, 4555–4564.

[10] J. A. Dean, N. A. Lange, in *Lange's Handbook of Chemistry*, 15 ed., McGraw-Hill Professional Publishing, New York, **1998**, pp. 4.41-44.53.

[11] D. Munz, K. Meyer, *Nat. Chem. Rev.* **2021**, *5*, 422–439.

[12] a) T. Ochiai, D. Franz, S. Inoue, *Chem. Soc. Rev.* **2016**, *45*, 6327–6344; b) L. F. B. Wilm, T. Eder, C. Mück-Lichtenfeld, P. Mehlmann, M. Wünsche, F. Buß, F. Dielmann, *Green Chem.* **2019**, *21*, 640–648.

[13] a) M. Tamm, S. Randoll, T. Bannenberg, E. Herdtweck, *Chem. Commun.* **2004**, 876–877; b) M. Tamm, D. Petrovic, S. Randoll, S. Beer, T. Bannenberg, P. G. Jones, J. Grunenberg, *Org. Biomol. Chem.* **2007**, *5*, 523–530; c) A. Doddi, M. Peters, M. Tamm, *Chem. Rev.* **2019**, *119*, 6994–7112; d) N. Kuhn, R. Fawzi, M. Steimann, J. Wiethoff, D. Bläser, R. Boese, *Z. Naturforsch. B* **1995**, *50*, 1779–1784; e) P. Raja, R. S, T. Ghatak, *Eng. Sci.* **2020**, *12*, 23–37.

[14] a) D. Sarkar, C. Weetman, D. Munz, S. Inoue, *Angew. Chem. Int. Ed.* **2021**, *60*, 3519–3523; *Angew. Chem.* **2021**, *133*, 3561–3565; b) L. Pu, M. M. Olmstead, P. P. Power, B. Schiemenz, *Organometallics* **1998**, *17*, 5602–5606; c) Brian P. Johnson, S. Almstätter, F. Dielmann, M. Bodensteiner, M. Scheer, *Z. Anorg. Allg. Chem.* **2010**, *636*, 1275–1285.

[15] a) R. S. Simons, L. Pu, M. M. Olmstead, P. P. Power, *Organometallics* **1997**, *16*, 1920–1925; b) P. Wilfling, K. Schittelkopf, M. Flock, R. H. Herber, P. P. Power, R. C. Fischer, *Organometallics* **2015**, *34*, 2222–2232.

[16] a) G. Ossig, A. Meller, S. Freitag, R. Herbst-Irmer, *J. Chem. Soc. Chem. Commun.* **1993**, 497–499; b) T. Fjeldberg, H. Hope, M. F. Lappert, P. P. Power, A. J. Thorne, *Chem. Commun.* **1983**, 639–641.

[17] a) A. D. Bage, T. A. Hunt, S. P. Thomas, *Org. Lett.* **2020**, *22*, 4107–4112; b) K. Fujiwara, S. Yasuda, T. Mizuta, *Organometallics* **2014**, *33*, 6692–6695.

[18] M. Muhr, P. Heiß, M. Schütz, R. Bühler, C. Gemel, M. H. Linden, H. B. Linden, R. A. Fischer, *Dalton Trans.* **2021**, *50*, 9031–9036.

[19] a) D. Franz, E. Irran, S. Inoue, *Dalton Trans.* **2014**, *43*, 4451–4461; b) M. M. Melzer, S. Jarchow-Choy, E. Kogut, T. H. Warren, *Inorg. Chem.* **2008**, *47*, 10187–10189.

Manuscript received: August 22, 2022
Revised manuscript received: August 22, 2022
Accepted manuscript online: August 23, 2022
Version of record online: September 20, 2022